Coastal Marine Science 36(1): 1–12, 2013

Numerical modeling of tidal dynamics in the Java Sea

Mustaid Yusuf[1]* and Tetsuo Yanagi[2]

[1] *Department of Earth System Science and Technology, Interdisciplinary Graduate School of Engineering Sciences, Kyushu University, Kasuga 816–8580, Japan. E-mail:mustaid@riam.kyushu-u.ac.jp*
** Faculty of Science, Mulawarman University, Samarinda, Indonesia.*
[2] *Research Institute for Applied Mechanics, Kyushu University, Kasuga 816–8580, Japan*

Received 17 May 2012; Accepted 17 October 2012

Abstract — Numerical experiments have been performed to study the characteristic of tide and tidal current in the Java Sea using the new version of COHERENS (*Coupled Hydrodynamical-Ecological model for Regional and Shelf Seas*), COHERENS V2.0. In the present study we focus on the tidal wave propagation, tidal energy propagation, tide-induced residual current and the tidal front critical value in the Java Sea. Based on our model results, we have found that tidal wave and tidal energy fluxes propagate westward in the Java Sea and also clearly shown the bifurcation of M_2 tidal wave in the Makassar Strait. K_1 tidal energy flux is coming from the Pacific Ocean while M_2 tidal energy flux is from the Indian Ocean. Tidal waves loss their energy when entering the Java Sea due to the steep bottom topography in the inlet (eastern part). Tide-induced residual current generated by K_1 tide shows a remarkable counterclockwise rotational flow due to geometrical boundary effect and bottom topography despite a clockwise flow by M_2 tide in the western part due to the bottom topography and shoaling effect. Comparison between the value of $\log(H/U^3)$, where H is the water depth in m and U is the amplitude of tidal current in m s^{-1}, with the composite image of MODIS-aqua and MODIS-tera of SST gradient distribution for transitional (wet to dry) season in the Java Sea reveals that the tidal front is located at $\log(H/U^3)$ value of 3.5.

Key words: tide, tidal current, tidal front, tidal energy, tide-induced residual current, numerical model

Introduction

The Java Sea is a primary water body in the western part of the Indonesian Waters as it connects three main islands in Indonesia, i.e., Java, Kalimantan and Sumatera Islands. This condition also makes the Java Sea receiving great pressure on its environment from three islands. Prior to study further about its environment, a comprehensive knowledge about the physical processes acting on the Java Sea is required. The knowledge on the physical conditions in the coastal sea is indispensable for the correct biological and chemical understanding of oceanographic phenomena (Yanagi 2011). It is well known that tide and tidal current play an important role in the shallow and narrow shelf seas such as the Java Sea (Simpson and Hunter 1974, Guo and Yanagi 1994, Hatayama et al. 1996).

Several previous studies about the tide and tidal current in the Indonesian Seas by means of numerical modeling have been conducted. Hatayama et al. (1996), using two-dimensional hydrodynamic model, have investigated the tidal currents in the Indonesian Seas and their effect on mixing and transport. They described that M_2 tide in the Java Sea is coming from the Indian Ocean through the Flores Sea and the Malacca Strait, while K_1 tide is coming from the Pacific Ocean through the Makassar Strait. They also noticed that tidal front is formed in the southwestern part of the Makassar Strait, as well as in the Java Sea by calculating the Simpson's parameter (Simpson et al. 1978) using the M_2 and K_1 tidal currents. Another study about tidal circulation and mixing over the Java Sea has been conducted by Koropitan and Ikeda (2008) using three-dimensional hydrodynamic model combined with observation data. They found that tidal mixing intensification occurs in the central part of the Java Sea and also found the appearance of tidal front in that region. The characteristic of K_1 and M_2 tidal current in the Indonesia Seas is also briefly overviewed by Ray et al. (2005) based on the data assimilation work of Egbert and Erofeeva (2002). They have shown the co-tidal and co-range charts and also the mean barotropic energy flux vectors for K_1 and M_2. Zu et al. (2008) also have shown the energy flux vectors around the Indonesia Seas in relation with their focus of study, the East China Sea. However, all the authors have no detail descriptions about the tidal front and tidal energy propagation particular in the Java Sea.

In the present study we focus on the characteristic of tide and tidal current in the Java Sea with emphasizing on tidal wave and tidal energy propagation as well as tidal front formation. Comparing with the previous authors, we also applied 3D barotropic hydrodynamic model, 2-minute resolution of horizontal grid size (the same resolution with Koropi-

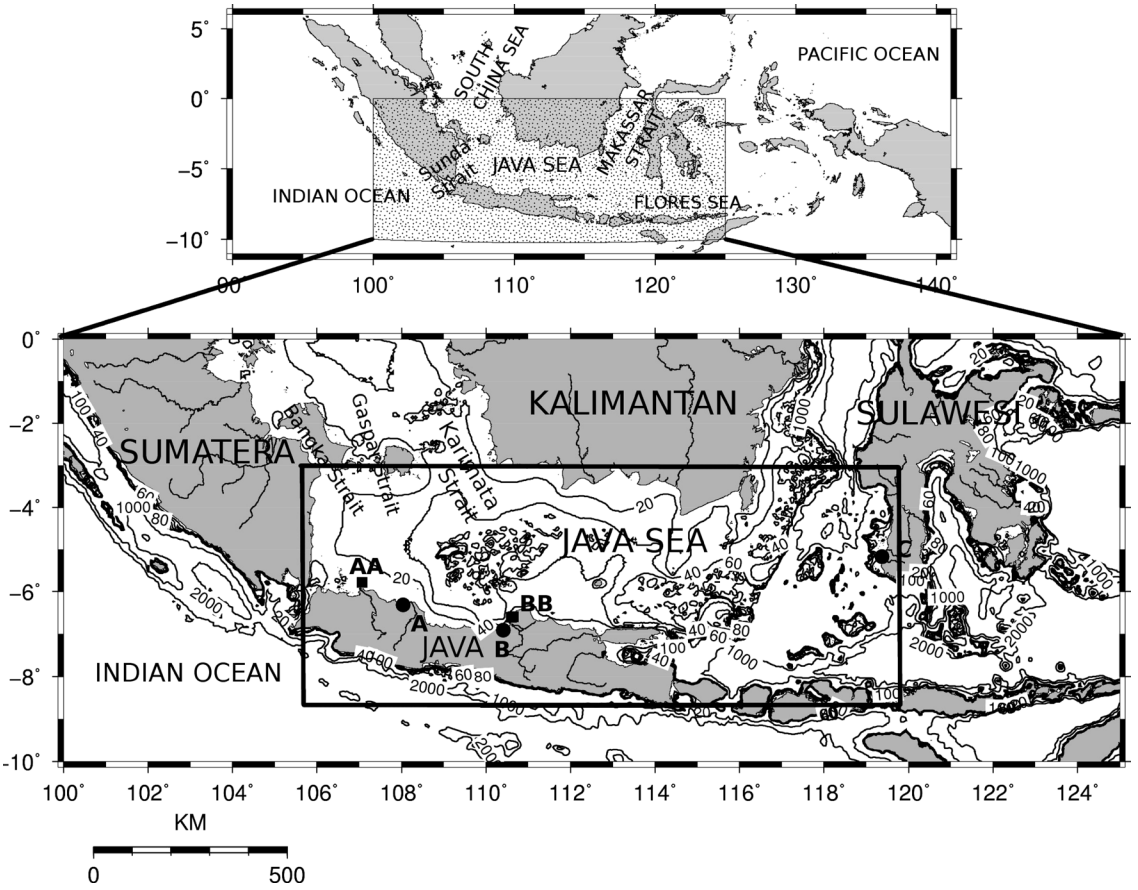

Fig. 1. Indonesia Waters (upper figure) and model domain (lower figure marked by solid line). Observation points of tide gauge (denoted by solid circle) A=Indramayu, B=Semarang and C=Makassar. Current Measurement points (denoted by solid square) AA=Karawang and BB=Jepara. Contour number indicates depth in meter.

tan and Ikeda (2008)), but we extended the model area to the east including the southern part of the Makassar Strait and the western part of the Flores Sea (Fig.1). The extension of the model area is intended to get a full overview of the Java Sea and to calculate the influence of the adjacent waters in particular the Makassar Strait and the Flores Sea.

Materials and Methods

Geography and morphology of the Java Sea

The Java Sea is situated in the western part of Indonesian Waters over the Sunda shelf. The Java Sea is connected to the Indian Ocean through the Sunda Strait, connected to the East China Sea through Karimata, Gaspar and Bangka Straits and directly connected to the Makassar Strait which is known as the main passage of Indonesian Throughflow (Fig. 1).

The morphology of the Java Sea is roughly parallelogram, which is bordered by the Kalimantan Island on the north, Sumatera Island on the west and Java Island on the south, but there is no lateral boundary on the east. The depth of the Java Sea increases from about 20 m off the coast of South Sumatera to more than 60 meters in its eastern part (Wyrtky 1961).

Observation data

There are three tide gauge stations i.e. Indramayu, Semarang and Makassar, whereas two locations for current station, i.e. Jepara and Karawang. Locations of those stations are depicted in Fig. 1. Sea level data are obtained from BAKOSURTANAL (National Coordination Agency for Surveys and Mapping) at Makassar and Semarang, whereas that at Indramayu as well as current data are obtained from BROKDKP (Institute for Marine Research and Observation).

Numerical model

The hydrodynamic model COHERENS (*Coupled Hydrodynamical-Ecological model for Regional and Shelf Seas*) is a three-dimensional multi-purpose numerical model, designed for application in coastal and shelf seas, estuaries, lakes and reservoirs (Luyten 2011). COHERENS V2.0, the new version of COHERENS, is applied for this study.

Barotropic mode of COHERENS V2.0 with eight major tidal constituents (M_2, K_2, S_2, N_2, K_1, O_1, P_1 and Q_1) along the open boundary as generating force is applied to simulate

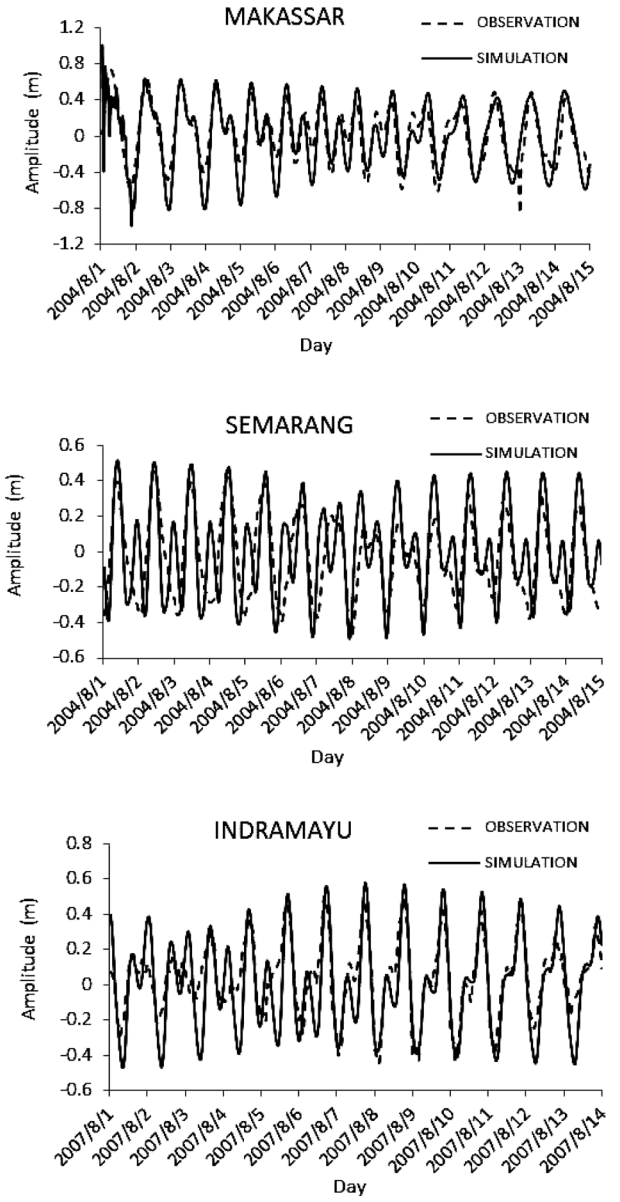

Fig. 2. Verification of tidal elevation.

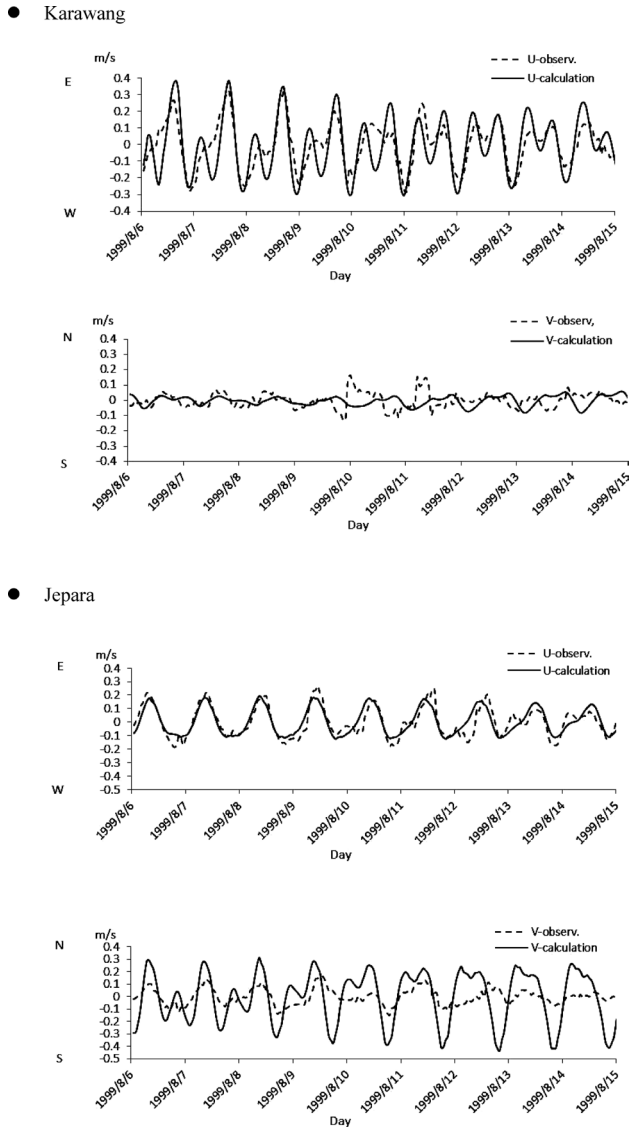

Fig. 3. Verification of tidal current.

the tide and tidal current in the Java Sea. The harmonic constants of those tidal constituents along the open boundary are taken from NAO99b (Matsumoto et al. 2000).

Model domain of this study spreads on 3.036°S–8.673°S of latitude and 105.675°E–119.808°E of longitude (Fig. 1). The model area has been divided into 425×170 grids in horizontal and 20 layers of non-uniform sigma coordinate in the vertical. Bathymetry input of the model was taken from the ETOPO2v2 (National Geophysical Data Center, NOAA, U.S. Department of Commerce, http://www.ngdc.noaa.gov/). The horizontal grid spacing is $\Delta x=\Delta y=2'$ (3.704 km).

TVD (Total Variation Diminishing) scheme using the superbee limiter as a weighting function between the upwind scheme and either the Lax-Wendroff scheme in the horizontal or central scheme in the vertical is applied to the advection scheme of 2D and 3D currents. This scheme is chosen due to the advantage of TVD in combining the monotonicity of the upwind scheme with the second order accuracy of Lax-Wendroff scheme (Luyten 2011). Smagorinsky formulation is applied for the horizontal diffusion coefficient with Smagorinsky coefficients for momentum and scalar is 0.2 either spatially uniform roughness length 0.0035 is used for the bottom drag coefficient formulation.

Results and Discussion

Verification of elevation and current velocity

Tidal elevation from model results and observation data of three tide gauge stations are plotted as shown in Fig. 2. Comparison of the observation data and model results for elevation with the corresponding period (1st–15th, August

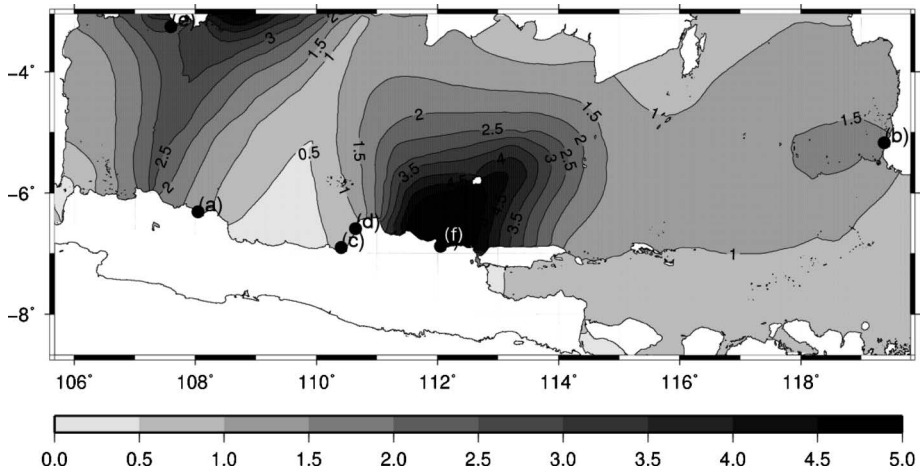

Fig. 4. Distribution of $(K_1+O_1)/(M_2+S_2)$.

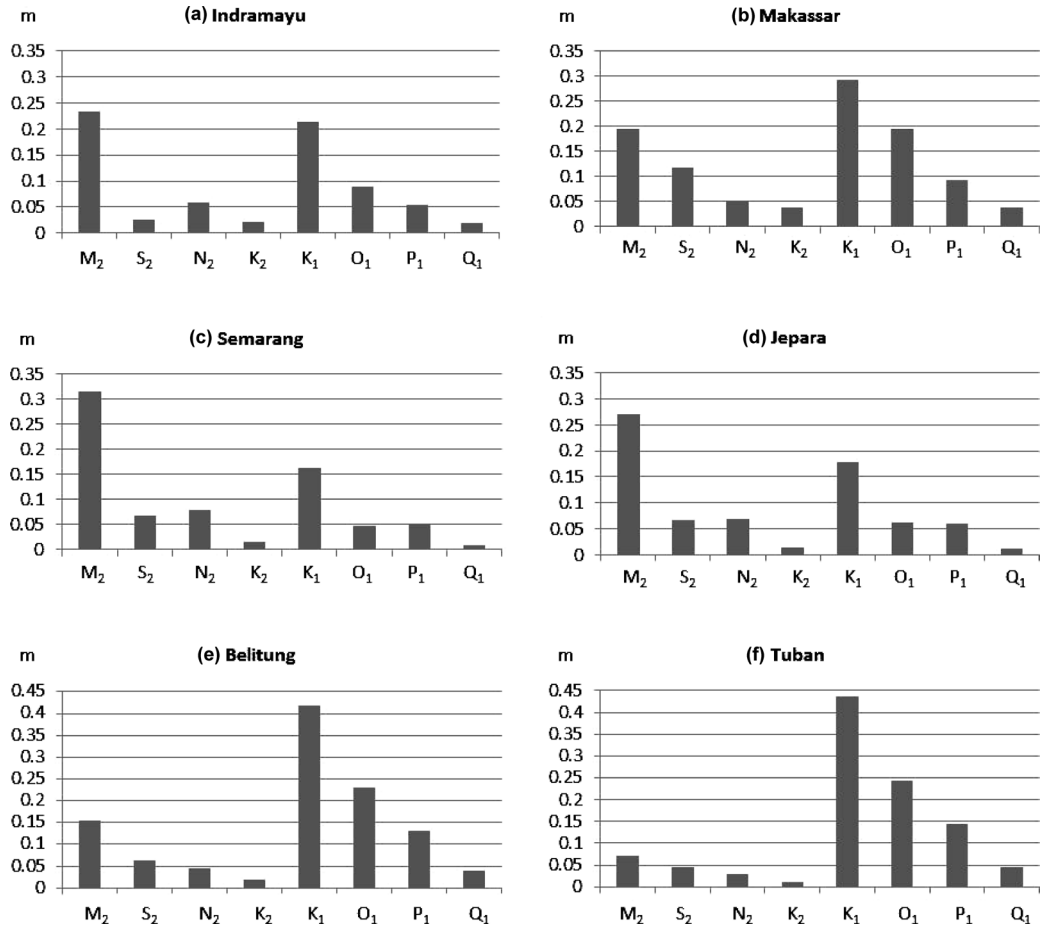

Fig. 5. Calculated amplitude spectrum distribution of major tidal components.

2004 for Semarang and Makassar; 1st–14th, August 2007 for Indramayu) is made to check the quality of the model results (different period is due to the observation data availability). From the comparison at all points, the model results have a good agreement with the observation data in term of phase but there is slightly difference of the amplitude where model results have a slightly larger amplitude than the observation data. The difference is presumably due to the large dissipation of the kinetic energy caused by the large vertical eddy viscosity coefficient (the same problem have pointed out by Guo and Yanagi (1994)) and also the location of the tide gauge stations which are located very near to the coastline,

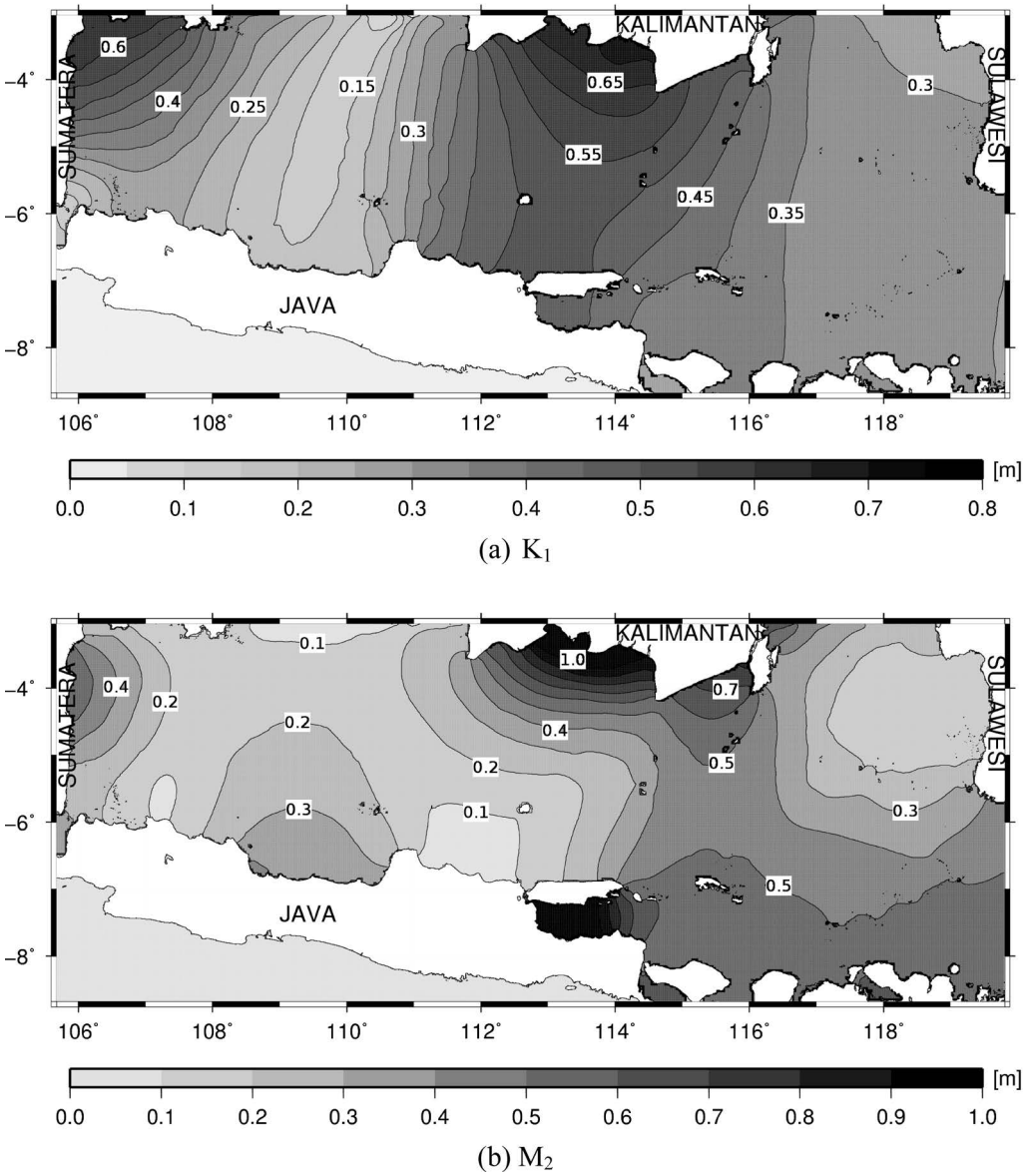

Fig. 6. Co-range charts of K_1 and M_2 tidal amplitude (unit is meter).

therefore it is very difficult to resolve well by this model resolution.

Verification for current is also performed in the period of 6th–15th, August 1999. There are two points of verification, i.e. Jepara and Karawang. The model results and the observation data are plotted as shown in Fig. 3. Prior to verification, 48-hours tide killer filter (Hanawa and Mitsudera 1985) has applied to the current data to eliminate the non-tidal current. In general, model results have a good agreement with the observation data especially for East–West component (U-Component), but there is difference in North-South component (V-component) as shown in Fig. 3. The amplitude of V-component is larger than the observation data. We suppose that the discrepancy is caused by the no slip condition at the sea bed which leads to a large velocity gradient near the sea bed in the vertical direction and then leads to a large sea bed friction (Guo and Yanagi 1994) and the grid resolution that we used in the model is not good enough to resolve the micro-scale geometry which gives a big effect to the tidal current, especially in the nearshore location.

Tidal type

As the previous authors (Wyrtky 1960, Koropitan and Ikeda 2008) have already noticed about the tidal type of the Java Sea, Fig. 4 shows the map of the ratio between principal diurnal and semi-diurnal tidal constituents, $(K_1+O_1)/(M_2+S_2)$ calculated by our model. We can understand that semi-diurnal constituents are dominant near the southern tip of Kalimantan and the northern coast of Central Java. On the other hand, diurnal constituents are dominant almost in the whole region of the Java Sea, that is, the eastern coast of South Su-

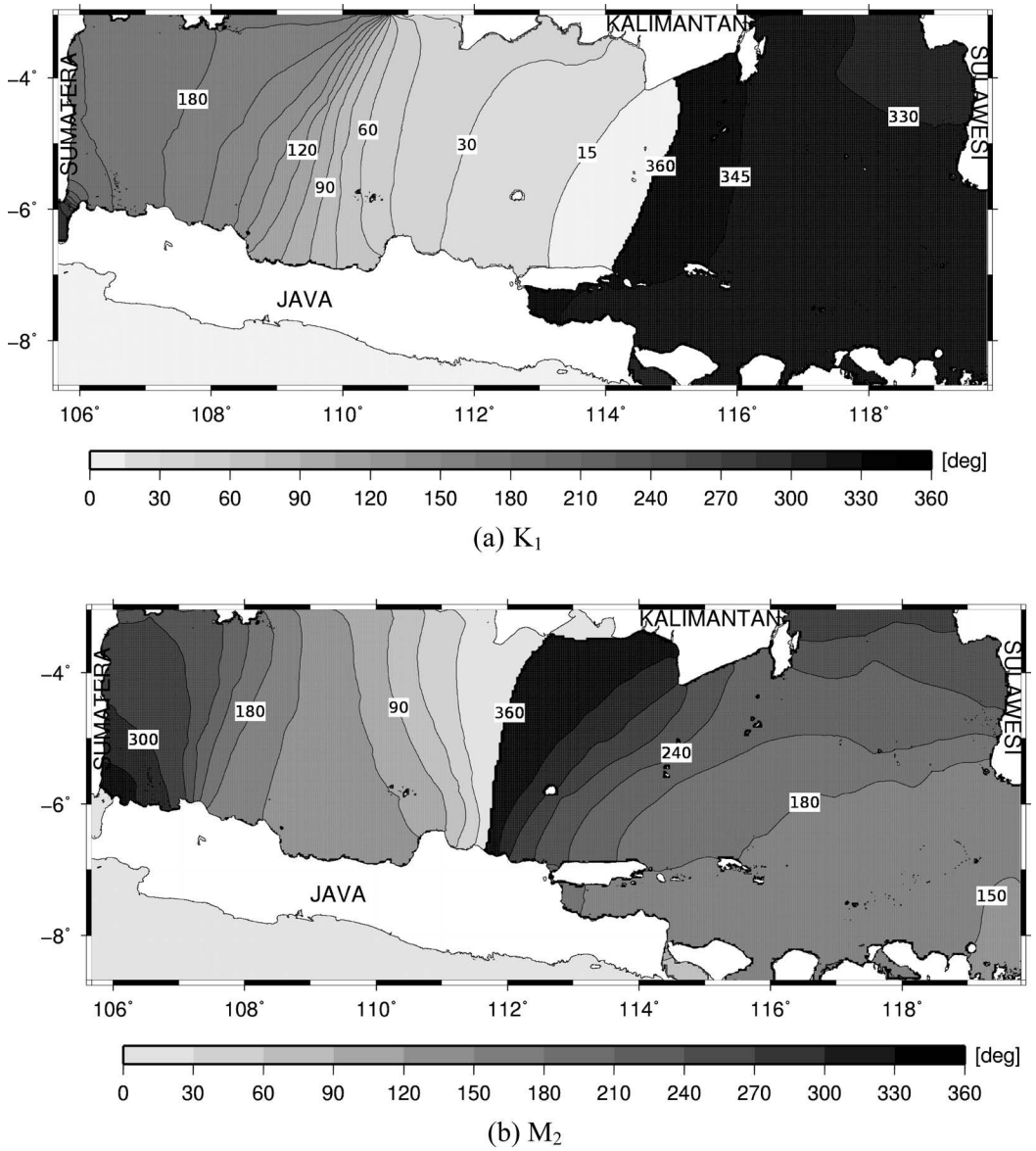

Fig. 7. Co-tidal charts of K1 and M2 tidal phase (unit is degrees referred to Indonesian mean time GMT+8 hours).

matera, the central part of the Java Sea and the northern coast of East Java (Fig. 5). The domination of the diurnal tides is due to the tidal waves resonance in the Java Sea. The natural oscillation period of the Java Sea is about 23.76 hours which is estimated from the formula $T=\frac{4}{3}L/\sqrt{gH}$, where L denotes the length of the Java Sea, 1100 km, and H the average depth, 30 m. This period is close to that of the K_1 tide.

Tidal wave propagation

Tidal wave propagates westward in the Java Sea. M_2 tidal wave is coming through the Flores Sea from the Indian Ocean while K1 tidal wave is coming through the Makassar Strait from the Pacific Ocean (Hatayama et al. 1996). Co-range and co-tidal charts of M_2 and K_1 constituents are shown in Fig. 6 and Fig. 7, respectively. Model results show that there is counterclockwise phase propagation of M_2 tidal wave in the Java Sea. The phase of tides is well known to propagate counterclockwise in the northern hemisphere and propagates clockwise in the southern hemisphere (Yanagi and Takao 1998). In the case of the Java Sea which is located in the southern hemisphere but the phase of M_2 tide propagates counterclockwise. The direction of the phase propagation is mainly governed by the large amplitude part of the incoming wave from the Flores Sea through the Makassar Strait. The large amplitude part propagates along the northern boundary (southern coast of Kalimantan Island). The same propagation type has been reported by Yanagi and Takao (1998) in the Gulf of Thailand which is located in the northern hemisphere but the semi-diurnal tide propagates clockwise, which is governed by the propagation of the large amplitude part of the incoming wave. Diurnal tide (K_1) as well as semi-diurnal tide (M_2) propagates from the eastern

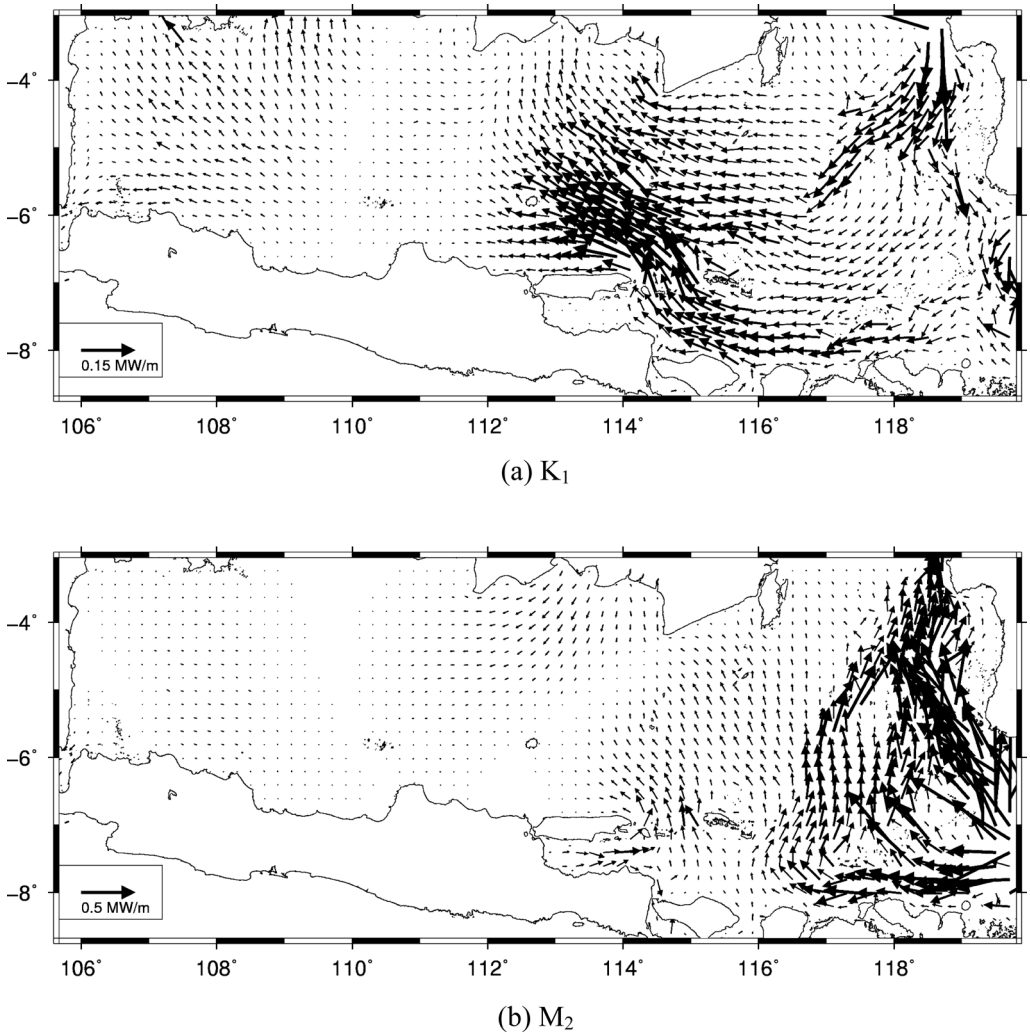

Fig. 8. Depth-integrated energy flux vectors for K_1 and M_2 tide during one tidal cycle.

part to the western part of the Java Sea.

It is clearly seen from the co-tidal charts (Fig. 7) that tidal wave propagates faster in the central southern part of the Java Sea (off the central Java island) rather than the central northern part of the Java Sea (off the Kalimantan island) due to the bottom topography of the Java Sea, where the southern part is deeper than the northern part. The bottom topography is also the reason of the difference of tidal amplitude distribution of K_1 as well as M_2 which are larger in the northern part rather than the southern part of the Java Sea (Fig. 6).

It is also seen that M_2 tide (Fig. 7b) from the Indian Ocean and the Flores Sea bifurcates in the Makassar Strait, with one propagating into the Java Sea and the other continuing northwards to the northern part of the Makassar Strait. On the other hand, K_1 tide propagates southward in the Makassar Strait and afterward it shifts into the Java Sea and continuing westwards to the western part of the Java Sea (Fig. 7a). Model results also show that diurnal component propagates slower than semi-diurnal component. Since the natural oscillation period of the Java Sea is close to the period of K_1 tide, so the reflected K_1 tidal wave will resonate with the incoming wave. Hence, the resonance decreases the wave speed on the node in the central part of the Java Sea. It is seen from the dense line of K_1 tidal phase on the co-tidal chart of K_1 (Fig. 7a). These results are similar to the previous authors (Ray et al. 2005, Koropitan and Ikeda 2008).

Tidal energy propagation

The previous authors (Ray et al. 2005, Zu et al. 2008) have shown the tidal energy propagation in the Indonesian Seas for K_1 and M_2 tide. Ray et al. (2005) have found that the mean barotropic energy flux vectors for the K_1 tide propagate southward in the Makassar Strait while those for the M_2 tide propagate northward. Similar results are also shown by Zu et al. (2008). However, they did not describe it for the Java Sea.

In the present study, calculated results of the COHERENS model are analyzed to obtain the tidal energy balance using the equation (5.1). In the transformed and vertically integrated form, the model equations are written as follow

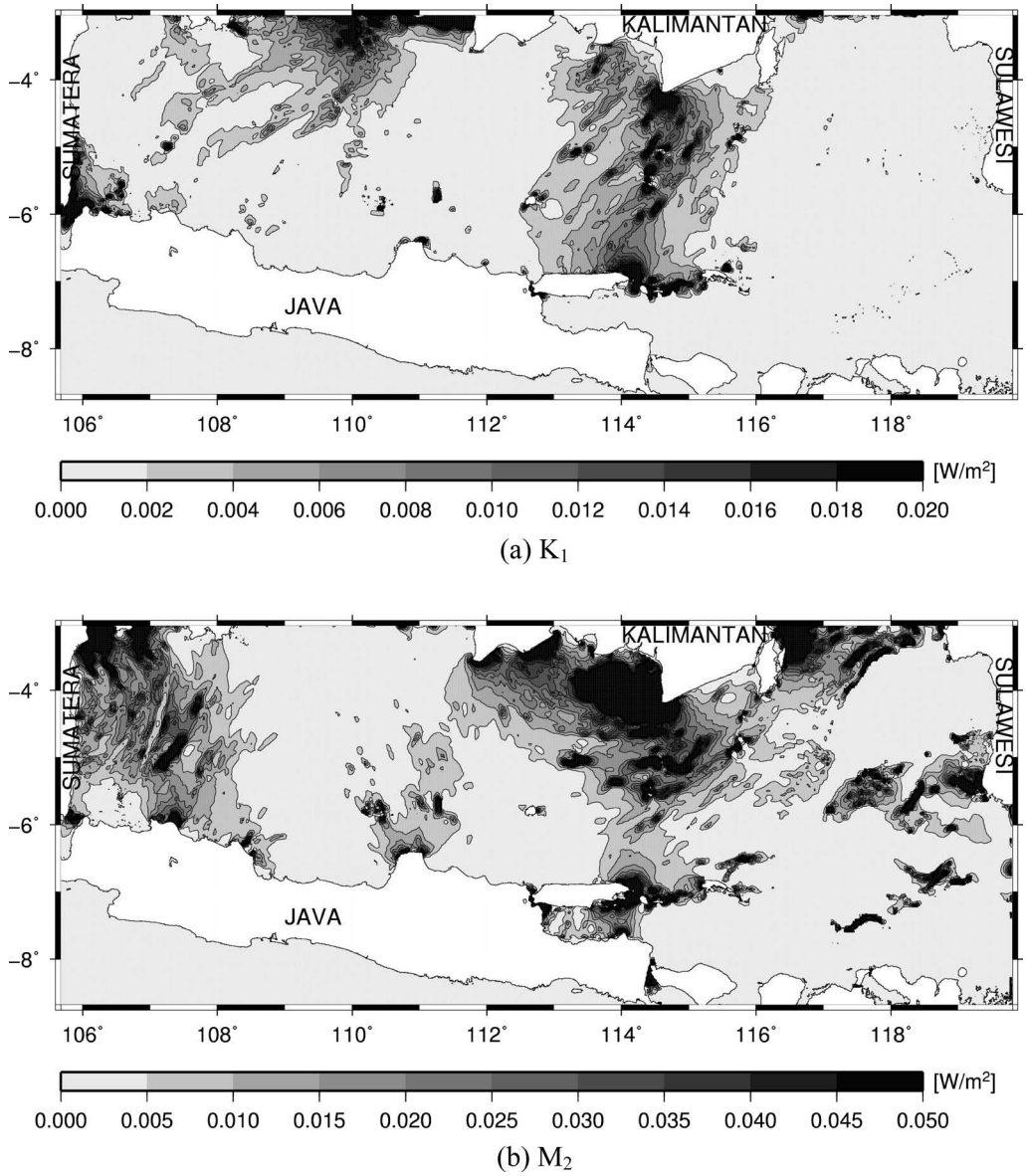

Fig. 9. Vertically integrated energy dissipation of K_1 and M_2 tide during one tidal cycle.

(Luyten 2011),

$$\frac{\partial}{\partial t}\left(\overline{E_k}+E_p\right)+\frac{1}{h_1h_2}\left[\frac{\partial}{\partial\xi_1}\left(h_2\overline{F_1}\right)+\frac{\partial}{\partial\xi_2}\left(h_1\overline{F_2}\right)\right]=\bar{D} \qquad (5.1)$$

where

$$\overline{E_k}=\frac{1}{2}\rho_0\int_0^{N_z}h_3\left(u^2+v^2\right)ds;\ E_p=\frac{1}{2}\rho_0 g\zeta^2$$

$$\left(\overline{F_1},\overline{F_2}\right)=\int_0^{N_z}h_3\left[\frac{1}{2}\rho_0\left(u^2+v^2\right)+\rho_0 g\zeta\right](u,v)ds$$

$$\bar{D}=\rho_0\left(u_s\tau_{s1}+v_s\tau_{s2}-u_b\tau_{b1}-v_b\tau_{b2}\right)-\rho_0\int_0^{N_z}\frac{\upsilon_T}{h_3}\left[\left(\frac{\partial u}{\partial s}\right)^2+\left(\frac{\partial v}{\partial s}\right)^2\right]ds$$

where E_k is the kinetic energy; E_p is the potential energy; D is the dissipation of energy by turbulent diffusion; h_1, h_2, h_3 is the grid spacing in the three (transformed) coordinate directions; ξ_1, ξ_2 is the orthogonal curviliniear coordinates. F_1, F_2 is the energy flux vector; (u_s, v_s) and (u_b, v_b) are the velocity respectively the surface and the bottom; (τ_{s1}, τ_{s2}) and (τ_{b1}, τ_{b2}) are the components of surface and bottom stress respectively; υ_T is vertical turbulent diffusion coefficient.

Our model results (Fig. 8) show that the energy flux vectors in the Makassar Strait are in accordance with the previous authors and we found that the tidal energy in the Java Sea propagates westward. It is clearly seen that the eastern part of the Java Sea is the inlet of the energy flux while the Sunda Strait is the outlet in the southern part as well as Karimata, Gaspar and Bangka are the outlet in the northern part. Energy flux vectors for the K_1 tide that propagate southward

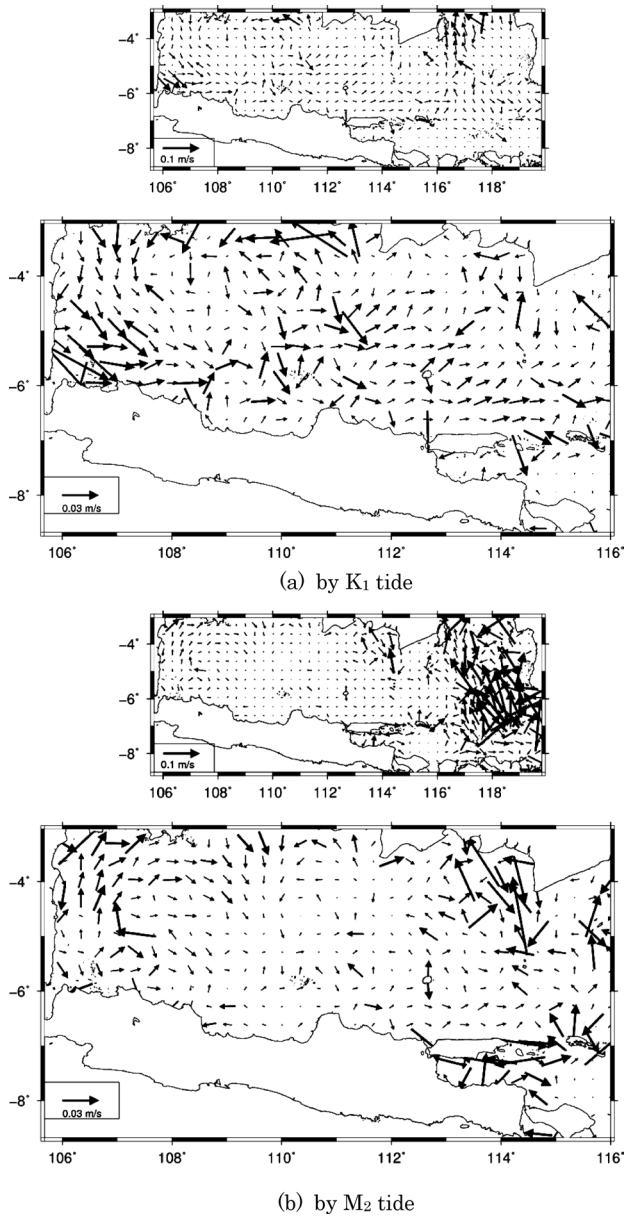

Fig. 10. Depth-mean tide–induced residual current. Upper figure shows the whole model area, lower figure shows more detail for the Java Sea.

in the Makassar Strait are shifted westward into the Java Sea. On the other hand, energy flux vectors for the M_2 tide are partially shifted westward into the Java Sea. K_1 and M_2 energy flux vectors indicate that the energy fluxes entering the Java Sea are coming from the Pacific Ocean and Indian Ocean. The loss of tidal energy while tidal waves entering the Java Sea, is indicated by the smaller magnitude of both K_1 and M_2 energy fluxes in the central part rather than those in the eastern part due to the steep bottom topography. Nevertheless, the magnitude of K_1 energy flux in the western part is larger due to the amplification in accordance with K_1 resonance period.

An interesting phenomenon appears in the Karimata Strait where Zu et al. (2008) have described that K_1 tidal energy flux vectors from the East China Sea propagate southward while our model result shows, in the northern part of the Java Sea, that the K_1 tidal energy flux vectors shift towards the Karimata Strait. Our model result shows that the large K_1 tidal energy dissipates on the southern tip of Karimata Strait (Fig. 9a). Nevertheless, the reason of the difference of ours and Zu et al. (2008) needs more detail study.

The distribution of vertically integrated energy dissipation for K_1 and M_2 tide in the Java Sea are shown in Fig. 9. It is clearly seen that the tidal energy fluxes are dissipated in the inlet while entering the Java Sea. In contrast with the K1 tidal energy flux (Fig. 9a), the M_2 tidal energy flux is dissipated in the western part of the Java Sea (Fig. 9b).

Tide-induced residual current

The information about the residual flow in the shelf seas is very important because it related with long-term material transport in that area. Even though the velocity of tidal residual flow is smaller than the tidal current but it plays more important roles for the long-term material transport. This phenomenon has been pointed out by Yanagi (1974), Zimmerman (1978) and others as reported by Yanagi and Yoshikawa (1983).

The flow pattern of the tide-induced residual current in the Java Sea, has been reported by Koropitan and Ikeda (2008). Nevertheless, they found a very complicated residual flow pattern of K_1 in the western part that is not agreed with the nature of tide-induced residual flow which forms a rotational flow pattern. The generation mechanisms of such rotational flow in relation to the tide-induced residual current have been described by Yanagi and Yoshikawa (1983) based on the previous result (Yanagi 1976, 1978, Oonishi 1977).

Fig. 10 shows our model results for the tide-induced residual current in the Java Sea generated by the K_1 and M_2 tide, respectively. The tide-induced residual current generated by the K_1 tide forms a counterclockwise rotational flow. The current flows westward in the northern part along the coast of Kalimantan and shifts to south in the western part along the east coast of Sumatera then shifts to east in the eastern part of the Java Sea along the north coast of Java, then shifts to north just when it reaches the Makassar Strait to complete the rotation. This flow pattern is formed due to geometrical boundary effect and bottom topography that correspond with the generation mechanisms described by Sugimoto (1975) and Yanagi and Yoshikawa (1983). Similar pattern also shown by the M_2, but a remarkable clockwise rotational flow appears in the western part. We suppose that the increasing of M_2 tidal amplitude due to the shoaling effect and solid boundary generates this pattern.

Tidal fronts

It is well known that tidal front is generated in the shelf

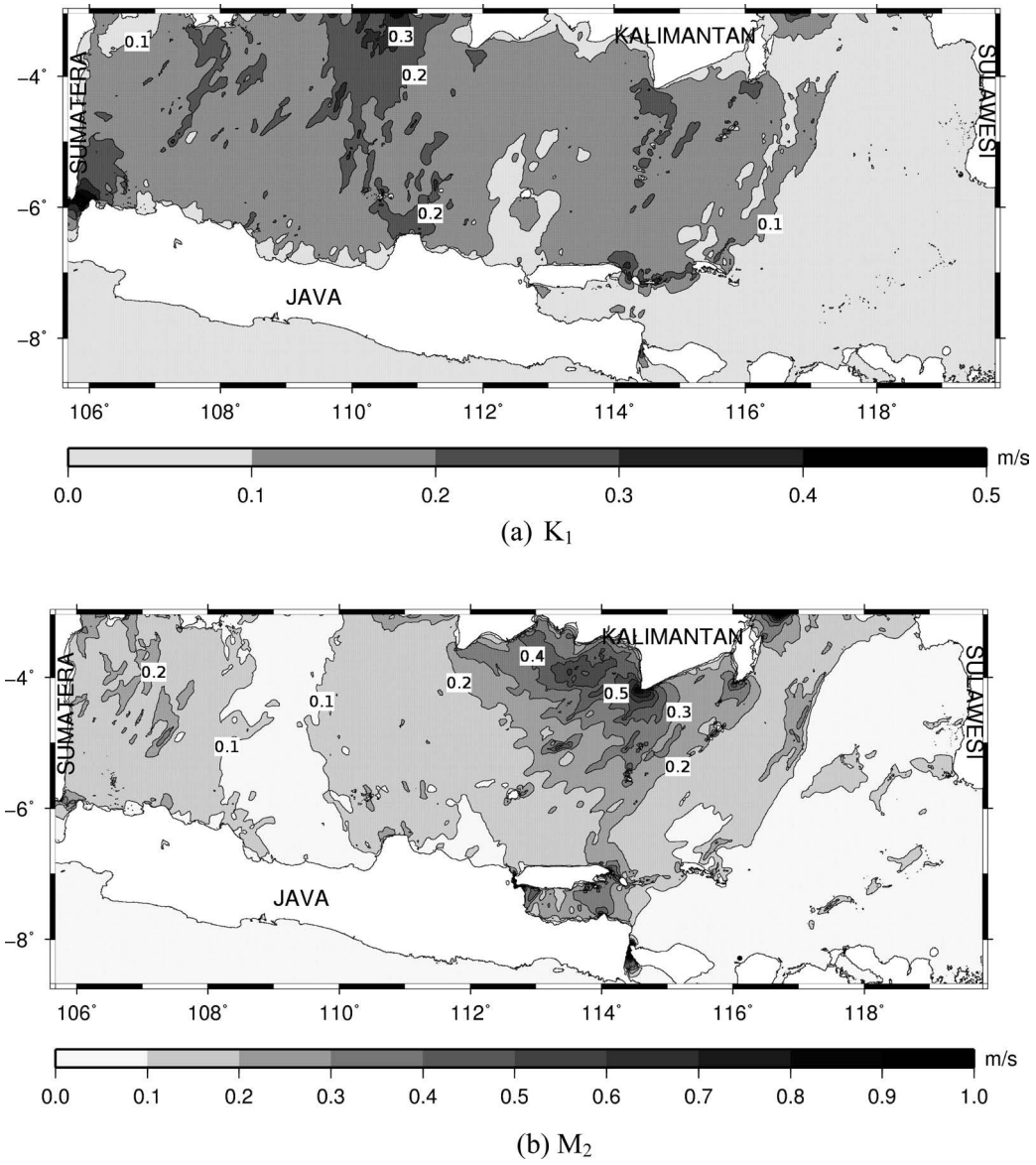

Fig. 11. Co-range chart of K_1 and M_2 tidal current amplitude

areas in summer, in a transition zone between vertically mixed water caused by tidal stirring and stratified water caused by heating through the sea surface (Yanagi and Koike 1987). Tidal front in the shelf seas has already been studied by many authors (e.g. Simpson and Hunter 1974, Yanagi and Koike 1987, Yanagi and Takahashi 1988). Such tidal front coincides with the value of $\log(H/U^3)$, where H is the water depth in m and U is the amplitude of tidal current in $m\,s^{-1}$, and known as 'critical value' (Sun and Isobe 2008). In the present study we calculate the $\log(H/U^3)$ value using the velocity component of M_2+K_1 to identify the tidal fronts in the Java Sea. The velocity component of M_2+K_1 was chosen based on the horizontal distribution of tidal current amplitude shown in Fig. 11.

Fig. 12 shows the isolines of the $\log(H/U^3)$. A composite image of several satellite images from MODIS-Aqua 4 km (4 micron night) on March year 2008, 2011 and MODIS-Tera 4 km (4 micron night) on March year 2009 (Fig. 13) shows the sea surface temperature distribution in the Java Sea. MODIS data used in this study were produced with the Giovanni online data system, developed and maintained by the NASA GES DISC (Acker and Leptoukh 2007). The image shows the temperature front in the northern part of the Java Sea along the southern coast of Kalimantan as well as in the western part along the east coast of South Sumatera. Comparing the model result (Fig. 12) and the satellite image (Fig. 13), we found that the temperature front coincides with the 3.5 value of $\log(H/U^3)$. Thus, we conclude that the critical value for tidal front generation in the Java Sea is 3.5. This critical value is nearly the same with the results of previous

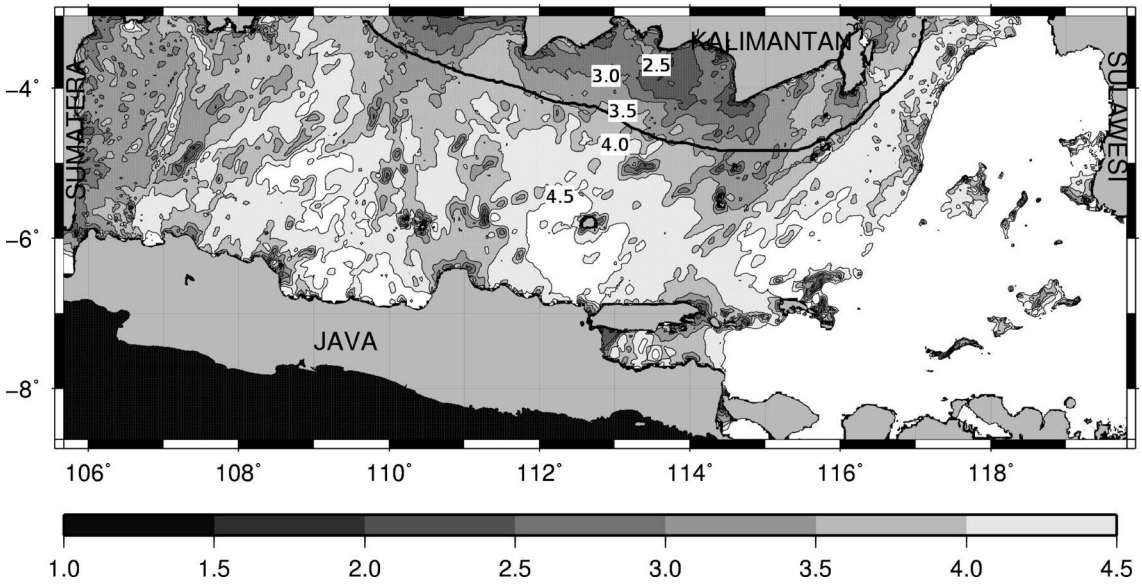

Fig. 12. Isoline of Log(H/U^3). White color denotes the value over than 4.5.

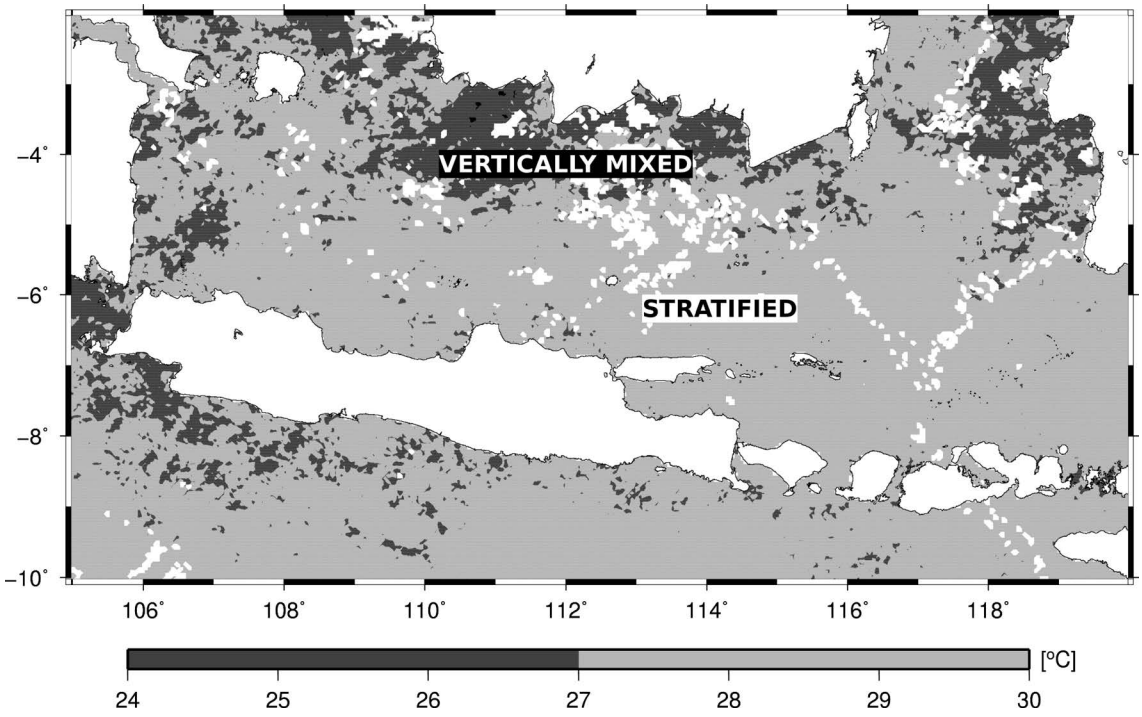

Fig. 13. Sea Surface Temperature distribution on nighttime of March, composite of MODIS-Aqua 4 km (4 micron night) in year 2008, 2011 and MODIS-Tera 4 km (4 micron night) in year 2009 images. White color on the sea indicates the clouds omission.

authors (Yanagi and Koike 1987, Yanagi and Takahashi 1988) in Osaka Bay, Japan that is 2.5–3.0 of log(H/U^3). In the case of the Java Sea, the same phenomenon appears that the front is formed along the transition zone and also separates the well-mixed nearshore region around Kalimantan Island from the stratified region of the center of the Java Sea.

Conclusions

In the present study we clearly show the westward propagation of the K_1 and M_2 tides in the Java Sea in agreement with the previous authors. We have shown that the K_1 tide is coming from the Pacific Ocean while M_2 tide is coming from the Indian Ocean. The tidal wave propagates faster in the southern part while the tidal amplitude is larger in the north-

ern part due to the bottom topography of the Java Sea. Tidal energy flux also propagates westward where the magnitude is decreased after entering the Java Sea, indicating the large energy loss at the inlet. Counterclockwise rotational flow of tide-induced residual current generated by the K_1 tide is due to the boundary geometry and topography effect while the clockwise rotational flow by the M_2 tide that appears in the western part is due to the bottom topography and shoaling effect. Tidal front is formed near the coastal water of Kalimantan. The critical value is found to be 3.5 of $\log(H/U^3)$, that is nearly the same with the values generally found in the other areas by the previous authors. It is clearly seen that the distribution pattern of M_2 tidal energy dissipation, tidal current amplitude and tidal front are coincided and related with each other. Based on the current results, we will examine more the consistency of the fronts by incorporating the wind driven current and the density driven current in the next study.

Acknowledgements

We would like to express our sincere thanks to Dr. Agus Setiawan, Director of Institute of Ocean Research and Observation and Dr. Ing, Khafid, National Coordination Agency for Surveys and Mapping, Indonesia, for the observation data. We acknowledge the MODIS mission scientists and associated NASA personnel for the production of the data used in this research. Our sincere thanks also dedicated to the two anonymous reviewer for their thoughtful comments and suggestions in improving this manuscript.

References

Acker, J. G. and G. Leptoukh. 2007. Online Analysis Enhances Use of NASA Earth Science Data, Eos, Trans. AGU 88: 14–17.

Egbert, G. D. and S. Y. Erofeeva. 2002. Efficient inverse modeling of barotropic ocean tides. J. Atmos. Oceanic Technol. 19: 183–204.

Guo, X. and T. Yanagi. 1994. Three Dimensional Structure of Tidal Currents in Tokyo Bay, Japan. La Mer 32: 173–185.

Hanawa, K. and H. Mitsudera 1985. On daily average of oceanographic data. Coastal Oceanographic Bull. 23: 79–87 (in Japanese).

Hatayama, T., T. Awaji and K. Akitomo. 1996. Tidal Currents in the Indonesian Seas and their effect on transport and mixing. J. Geophys. Res. 105: 12,353–12,373.

Koropitan, A. F. and M. Ikeda. 2008. Three-dimensional modeling of tidal circulation and mixing over the Java Sea. J. Oceanogr. 64: 60–80.

Luyten, P. 2011. COHERENS—A Coupled Hydroynamical-Ecological Model for Regional and Shelf Seas: User Documentation, Version 2.0, Royal Belgian Institute of Natural Sciences (RBINS-MUMM), Gulledelle 100, 1200 Brussels, Belgium.

Matsumoto, K., T. Takanezawa and M. Ooe. 2000. Ocean tide models developed by assimilating TOPEX/POSEIDON altimeter data into hydrodynamical model: A global model and a regional model around Japan. J. Oceanogr. 56: 567–581.

Oonishi, Y. 1977. A numerical study on the tidal residual flow. J. Oceanogr. Soc. Japan 33: 207–218.

Ray, R. D., G. D. Egbert and S. Y. Erofeeva. 2005. A brief overview of tides in the Indonesian Seas. *Oceanography* 18: 74–79.

Simpson, J. H. and J. R. Hunter. 1974. Fronts in Irish Sea. Nature 250: 404–406.

Simpson, J. H., C. M. Allen and N. C. G. Morris. 1978. Fronts on the continental shelf, J. Geophys. Res. 83: 4607–4614.

Sugimoto, T. 1975. Effect of Boundary Geometries on Tidal Currents and Tidal Mixing. J. Oceanogr. Soc. Japan 31: 1–4.

Wyrtky, K. 1961. Physical oceanography of the Southeast Asian Waters, NAGA Rep. 2, Scripps Inst. of Oceanogr., Univ. Calif., La Jolla, California; 195 pp.

Yanagi, T. 1974. Dispersion due to the residual flow in the hydraulic model. Cont. Geophysical Inst. Kyoto Univ., Japan 14: 1–10.

Yanagi, T. 1976. Fundamental study on the tidal residual circulation I. J. Oceanogr. Soc. Japan 32: 199–208.

Yanagi, T. 1978. Fundamental study on the tidal residual circulation II. J. Oceanogr. Soc. Japan 34: 67–72.

Yanagi, T. and K. Yoshikawa. 1983. Generation mechanisms of tidal residual circulation. J. Oceanogr. Soc. Japan 39: 156–166.

Yanagi, T. and T. Koike. 1987. Seasonal variation in thermohaline and tidal fronts, Seto Inland Sea, Japan. Continental Shelf Res. 7: 149–160.

Yanagi, T. and T. Takao. 1998. Clockwise phase propagation of semi-diurnal tides in the Gulf of Thailand. J. Oceanogr. 54: 143–150.

Yanagi, T. and S. Takahashi. 1988. A tidal front influenced by river discharge. Dyn. Atmos. Oceans. 12: 191–206.

Yanagi, T. 2011. Water circulation and material transport in the coastal areas and marginal seas of East and Southeast Asia, S. Nishida, M. D. Fortes and N. Miyazaki, eds., Coastal Marine Science in Southeast Asia—Synthesis report of the core university program of the JSPS: Coastal Marine Science (2001–2010)—Terrapub: 13–22.

Yuasa, I. and H. Ueshima. 1992. A tidal front in winter influenced by river discharge. J. Oceanogr. 48: 239–255.

Zimmerman, J. T. F. 1978. Dispersion by tide induced residual current vortices. *In* Hydrodynamics of Estuaries and Fjords. J. Nihoul (ed.), pp. 207–216, Elsevier, Amsterdam.

Zu, T., J. Gan and S. Y. Erofeeva. 2008. Numerical Study of the tide and tidal dynamics in the South China Sea. Deep-Sea Res. I 55: 137–154.